A

	Batf3$^{+/+}$					*Batf3*$^{-/-}$				
				# of TCRs					# of TCRs	
Population	n mice (n expts)	Cells x10^3 Mean (SE)	# of reads	>.01% in 1 sample	>30% mice in 1 condition	n mice (n expts)	Cells x10^3 Mean (SE)	# of reads	>.01% in 1 sample	>30% mice in 1 condition
Foxp3$^-$	11 (3)	1468 (107)	250040	11522	2269	12 (3)	1354 (331)	201475	12010	2164
Foxp3$^+$	9 (3)	62.4 (14)	398636	7882	896	9 (3)	67.9 (18)	469148	4155	316

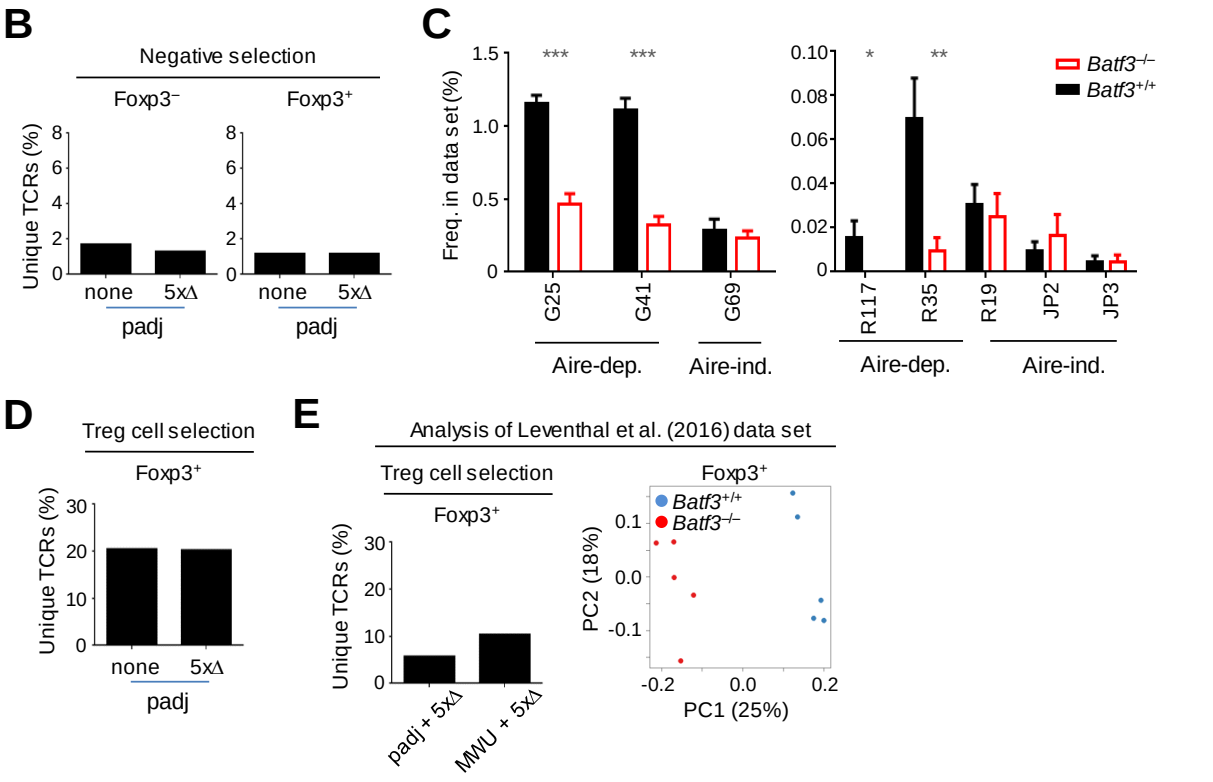

Figure S1. Related to Figure 1. Effects of BATF3-dependent CD8α$^+$ DCs on the TCR repertoire.

(A) Summary of TCR sequencing obtained from BM chimeras generated using TCliβ TCR transgenic *Tcra*$^{+/-}$ (*Batf3*$^{+/+}$ or *Batf3*$^{-/-}$) donors. After 8 weeks, Foxp3$^+$ Treg (CD4$^+$CD8$^-$Foxp3^{gfp+}) and Foxp3$^-$ Tconv (CD4$^+$CD8$^-$CD62L^{hi}CD24^{lo}Foxp3^{gfp-}) cells were sorted for TCR sequencing. Synthesis of TCRα cDNAs from purified T cells was performed using the Cα-specific primer 5'-GTGAATCAGGGCCAAC-3'. A two-step PCR was used to amplify multiple TRAV genes (multiplex PCR). Amplicons were purified after each PCR reaction using the Agencourt AMPure XP magnetic purification system. The ~200-600 bp amplicons were quantified using Qubit dsDNA BR assay kit (Invitrogen) and pooled in equimolar ratios for 250 bp paired end sequencing via the MiSeq platform (Illumina). Sequences were demultiplexed and analyzed using blastn to identify the TRAV and TRAJ gene segments using the IMGT database (Gludicelli

et al., 2006). This information was then used to determine the CDR3 sequence. A unique TCR was identified by its TRAV and CDR3 amino acid sequence. Data shown is the summary of sorting, sequencing, and filtering. Frequency filtering ("# of TCRs > .01%") keeps TCRs > 0.01% of raw data in any individual sample. Consistency filtering ("# TCRs > 30% of condition") keeps TCRs that were found in 30% of samples at > 0.01% frequency within an experimental condition defined by T cell subset and genotype.

(B) The unique number of negatively selected TCRs determined by the false-discovery rate adjusted *p* value (padj) with or without a 5-fold change criteria (5xΔ) of frequency filtered data (TCR in one sample > 0.01%) is shown. Padj was obtained using the R package DESeq2.

(C) The frequency in *Batf3*$^{+/+}$ and *Batf3*$^{-/-}$ TCR data sets of Treg cell TCRs previously identified to be BATF3- and AIRE-codependent (G25, G41, R117, R35) or -independent (G69, R19, JP2, JP3) in *in vivo* developmental studies (Perry et al., 2014) is shown.

(D) The unique number of Treg selected TCRs determined by the false-discovery rate adjusted *p* value (padj) with or without a 5-fold change criteria (5xΔ) of frequency filtered data (TCR in one sample > 0.01%) is shown. Padj was obtained using the R package DESeq2.

(E) Treg TCR sequence data from Leventhal et al. (2016) was analyzed using either the mRNA-Seq analysis method (DESeq2) or the same approach as in Figure 1D and 1E. **p* < .05, ***p* < .01, ****p* < .001, Student's t-test.

A

	Aire$^{+/+}$					*Aire*$^{-/-}$				
				# of TCRs					# of TCRs	
Population	n mice (n expts)	Cells x10^3 Mean (SE)	# of reads	>.01% in 1 sample	>30% mice in 1 condition	n mice (n expts)	Cells x10^3 Mean (SE)	# of reads	>.01% in 1 sample	>30% mice in 1 condition
Foxp3$^-$	9 (3)	734 (24)	130264	12587	1462	9 (3)	646 (20)	109055	14884	2158
Foxp3$^+$	7 (3)	31 (8)	396854	7587	640	7 (3)	21 (6)	142069	4745	372

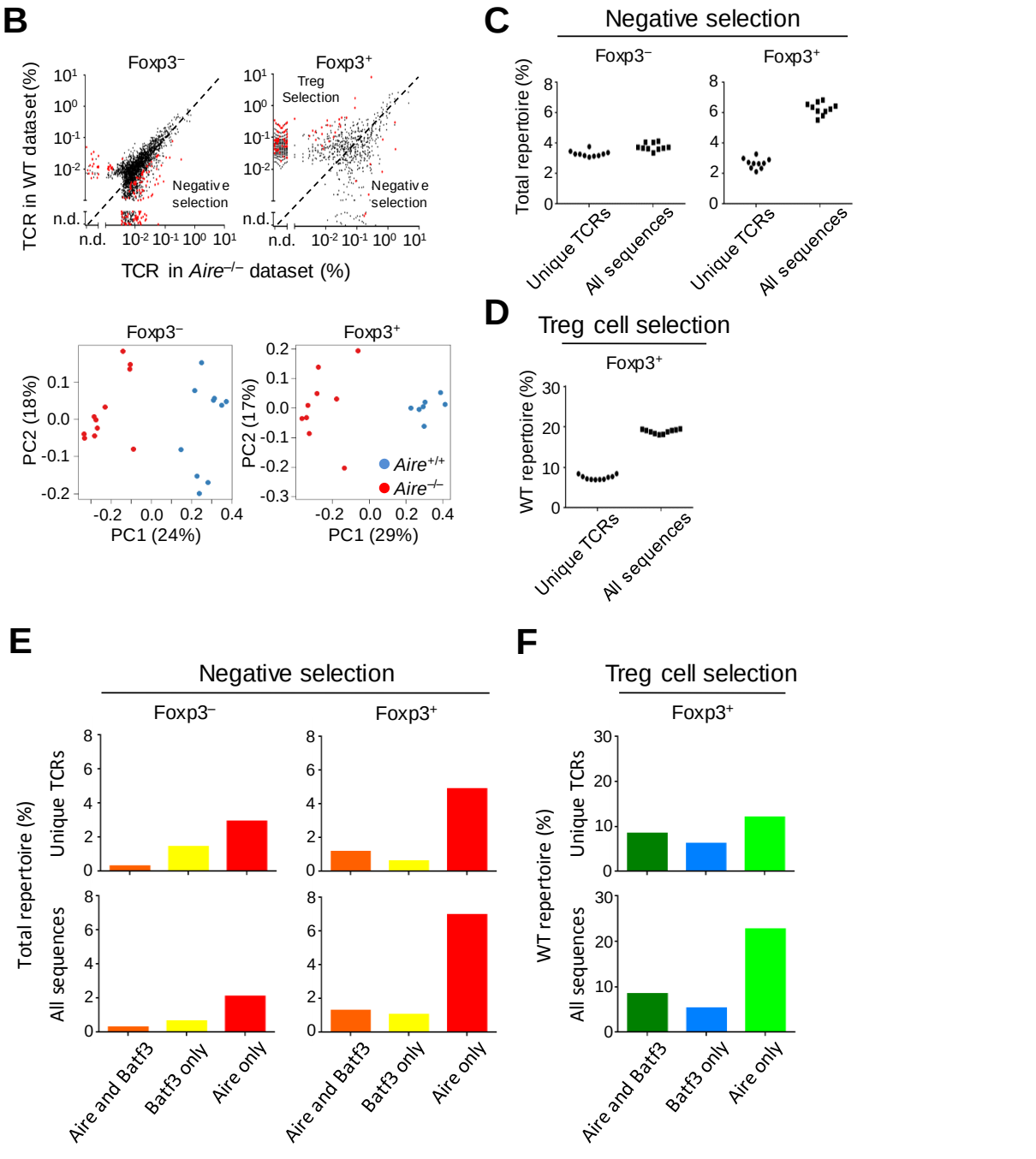

Figure S2. Related to Figure 1. Analysis of AIRE-dependent TCR repertoires.

(A) Summary of TCR sequencing of Foxp3^{-} Tconv or Foxp3^{+} Treg CD4SP cells from TCliβ^{+} transgenic → *Aire*$^{+/+}$ or *Aire*$^{-/-}$ BM chimeras as per Figure S1A.

(B) Top panel: Average TCR frequencies in the Foxp3^{-} and Foxp3^{+} AIRE data sets. Red dots indicate TCRs that are considered AIRE-dependent based on $p < .05$ (MWU) and 5-fold change as per Figure 1C. Bottom panel: PCA of Tconv and Treg cell TCR repertoires from *Aire*$^{+/+}$ (blue dots) and *Aire*$^{-/-}$ (red dots) BM chimeras.

(C,D) The percentage of unique TCRs or total sequences affected by the presence of AIRE on negative selection of the Foxp3^{-} and Foxp3^{+} TCR repertoire (C), and on Treg cell selection (D). Each dot represents a uniquely rarefied sample. All data sets were rarefied to the smallest sample size a total of ten times.

(E,F) Summary of the effect of BATF3 and AIRE on the total TCR repertoire for negative selection (E) and Treg cell selection (F). TCRs are identified as BATF3 and AIRE dependent based on Figure 1C.

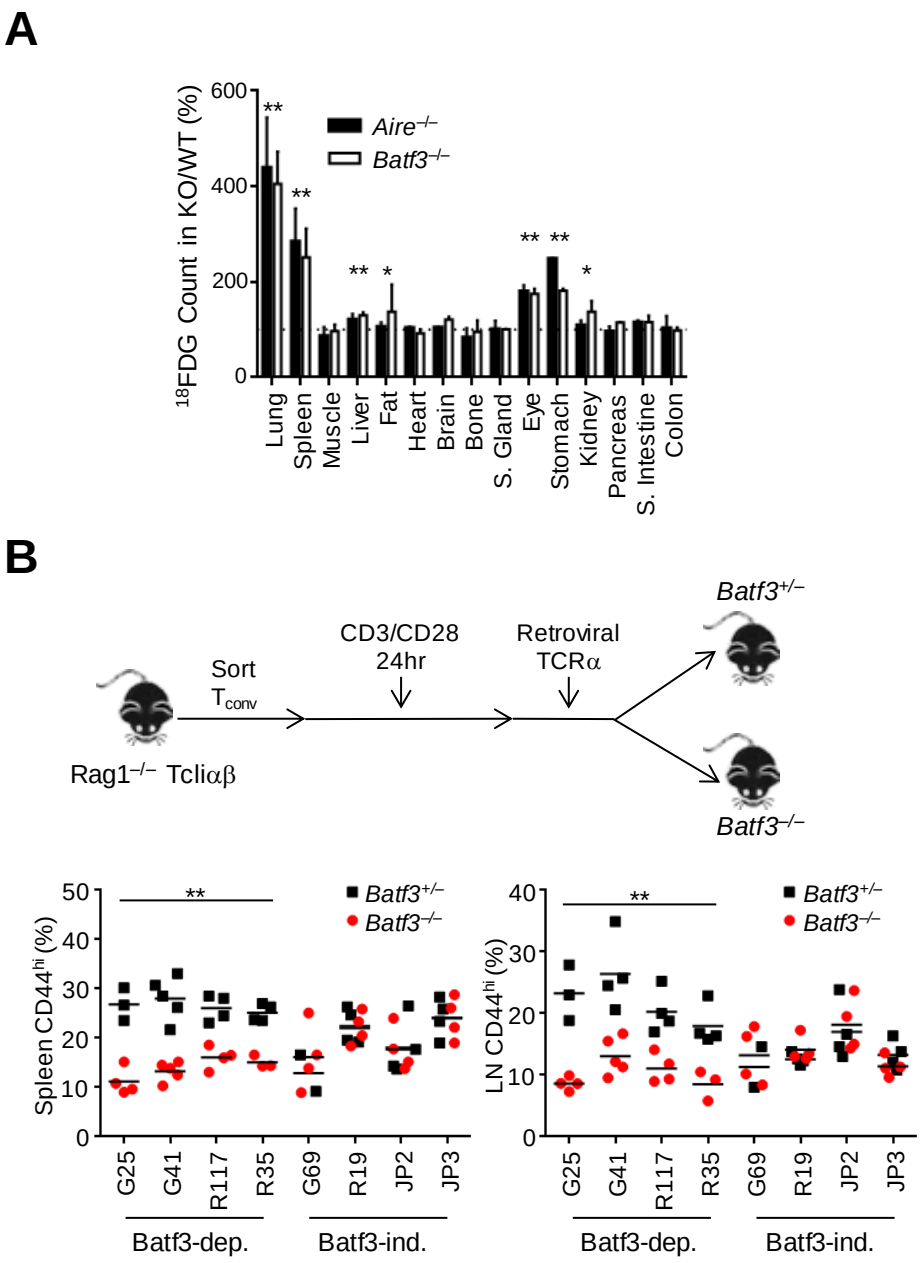

Figure S3. Related to Figure 2. Thymic tolerance by CD8α^{+} DCs prevents tissue-specific inflammation.

(A) ^{18}FDG uptake, a marker of inflammation, in tissues after transfer of mature Tconv and Treg cells from BATF3 or AIRE-deficient thymi into T-lymphopenic hosts. Experiment was performed as per Figure 2A, and the organs harvested and counted for radioactive uptake. Data is presented as per Figure 2C and includes tissues in that Figure for reference (mean + SEM).

(B) CD44 upregulation of T cells transduced with BATF3-dependent or -independent TCRs in *Batf3*$^{+/-}$ or *Batf3*$^{-/-}$ hosts. CD4^{+} T cells from TCli$\alpha\beta$ TCR transgenic mice were enriched and CD25-depleted using Automacs, then stimulated for 24h with plate bound CD3/CD28 antibody. T cells were retrovirally transduced (Hsieh et al., 2006) with the indicated TCRα chains and injected into 6-8 week old littermate-matched *Batf3*$^{+/-}$ and *Batf3*$^{-/-}$ mice. Spleens and pooled lymph nodes were harvested 11 days post injection and stained for CD44 as a marker of T cell activation. Transduced T cells were identified by a Thy1.1 reporter in the vector. Data is presented from each recipient, and was obtained in at least two independent experiments. **p* < .05, ***p* < .01, Student's t-test.

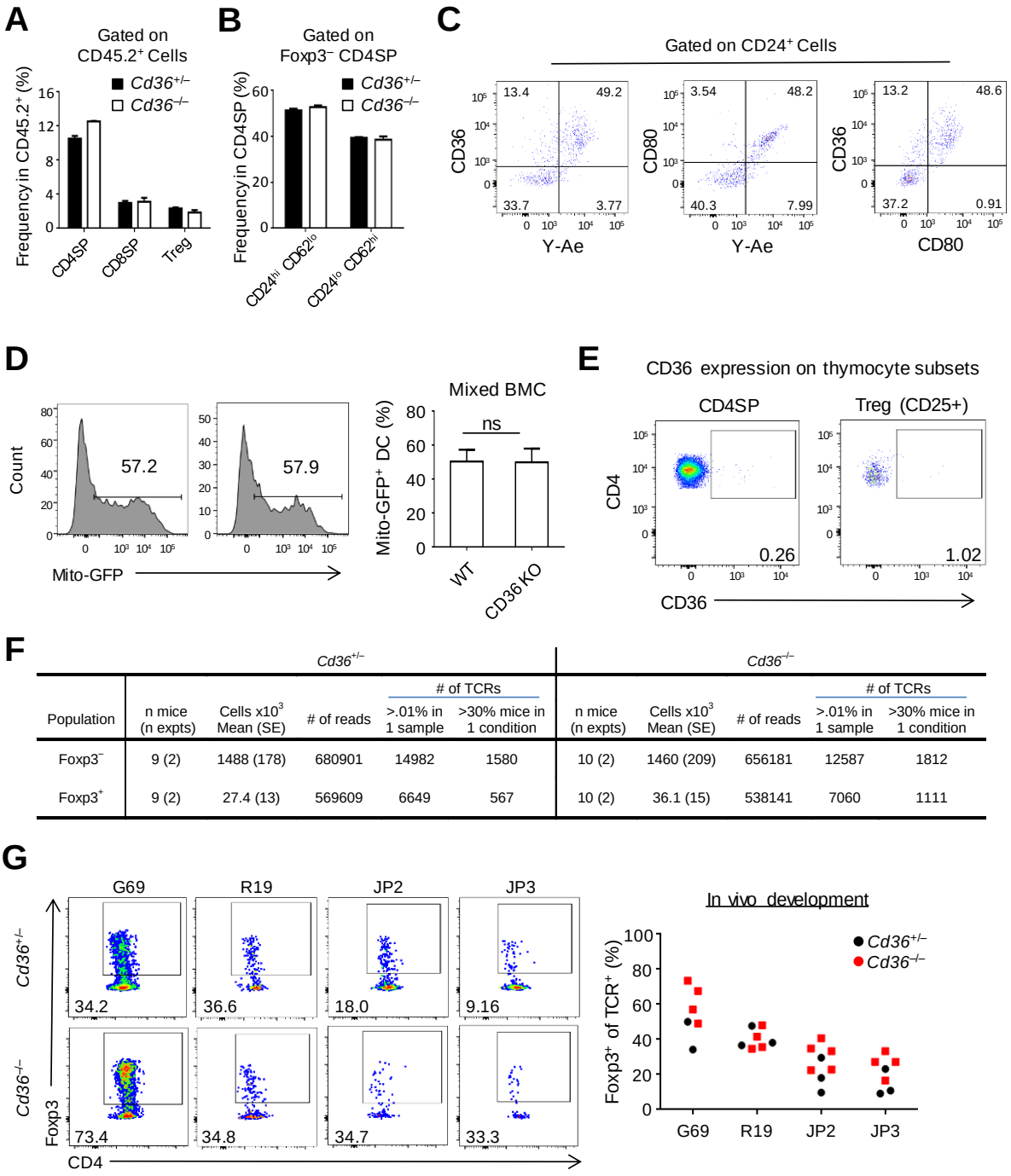

	Cd36+/–					Cd36–/–				
				# of TCRs					# of TCRs	
Population	n mice (n expts)	Cells x10^3 Mean (SE)	# of reads	>.01% in 1 sample	>30% mice in 1 condition	n mice (n expts)	Cells x10^3 Mean (SE)	# of reads	>.01% in 1 sample	>30% mice in 1 condition
Foxp3$^-$	9 (2)	1488 (178)	680901	14982	1580	10 (2)	1460 (209)	656181	12587	1812
Foxp3$^+$	9 (2)	27.4 (13)	569609	6649	567	10 (2)	36.1 (15)	538141	7060	1111

Figure S4. Related to Figure 4. Analysis of CD36-dependent TCR repertoires.

(A,B) Foxp3$^+$ CD4$^+$ (Treg), Foxp3$^-$ CD4$^+$ CD8$^-$ (CD4SP) and CD8$^+$ CD4$^-$ (CD8SP) thymocyte frequencies (A) or HSA^{lo} CD62^{hi} and HSA^{hi} CD62^{lo} CD4$^+$ frequencies (B) from TCliβ transgenic *Cd36*$^{+/–}$ or *Cd36*$^{–/–}$ → Ly5.1 BM chimeras. Data are presented as mean + SEM.

(C) Expression of CD36, CD80, and Eα:I-A^b (Y-Ae antibody) on $CD24^+$ (a.k.a. $CD8\alpha^+$) DCs from C57BL/6→Balb/c BM chimeras. Data are representative of two independent experiments with 2 mice per experiment.

(D) Representative FACS plots and summary graph of presence of mitochondrial-derived GFP (mito-GFP) in $CD8\alpha^+$ DCs from *Cd36*$^{+/-}$ or *Cd36*$^{-/-}$ → mito-GFP BM chimeras. Data are presented as mean + SD from two independent experiments with 1 replicate per condition.

(E) Representative FACS plots of thymocyte populations stained with CD36.

(F) Summary of TCR sequencing for CD36 BM chimeras as described in Figure S1A.

(G) *In vivo* Treg cell development of previously identified $CD11c^+$ DC-dependent BATF3 and AIRE-independent Treg TCRs (Perry et al., 2014) in *Cd36*$^{+/-}$ or $^{-/-}$ hosts. Each TCR was tested in at least two independent experiments with at least 1 replicate per condition. Summary data and representative FACS plots are shown. ***$p < .001$, Student's t-test.

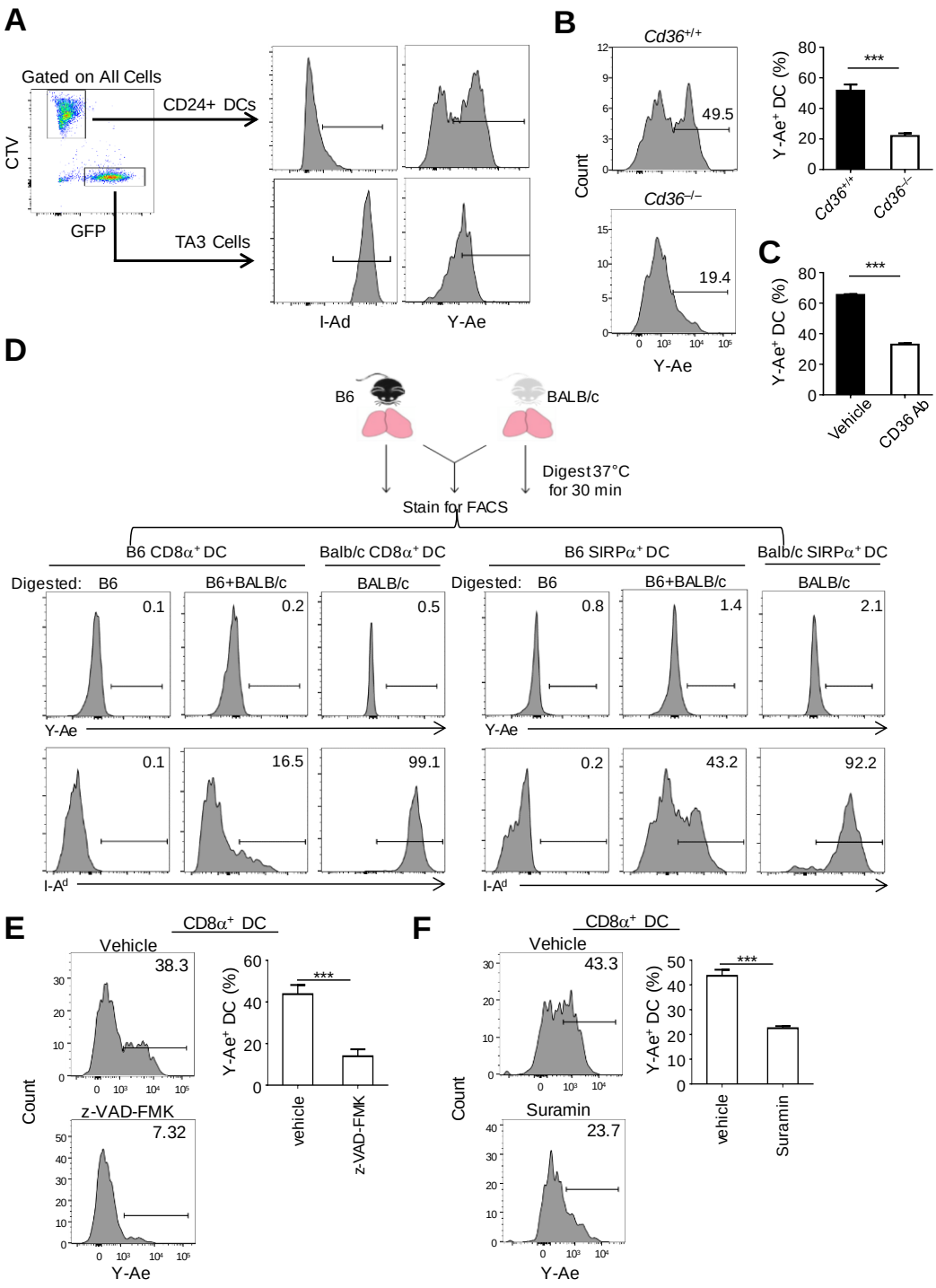

Figure S5. Related to Figure 5. Enzymatic digestion of the thymus can transfer cell surface MHC.

(A) Gating scheme for *in vitro* antigen transfer experiment. Cell trace violet (CTV) labeled $CD24^+$ bone marrow-derived DCs were co-cultured with GFP^+ TA3 cells at a 1:1 ratio for 6 hours. $CD24^+$ DCs expressed minimal GFP and $I\text{-}A^d$ whereas TA3 cells constitutively express GFP and

I-A^d but no CTV. TA3 cells are much larger and feature some non-specific autofluorescence for Y-Ae antibody that is at least a log order less than seen in $CD24^+$ DCs presenting Eα peptide on I-A^b.

(B) $CD11c^+$ DCs were MACS bead isolated from CD36-deficient or sufficient thymi and co-cultured *in vitro* with apoptotic GFP^+ TA3 cells at a 1:1 ratio for 6 hours to assess transfer of Eα. $CD11c^+$ I-Ab^+ $CD24^+$ DCs were analyzed for Eα presentation (Y-Ae^+ cells) via FACS. Shown are representative FACS plots and summary graph of two independent experiments with four replicates per experiment. ***$p < .001$.

(C) $CD11c^+$ DCs were MACS bead isolated from pooled C57BL/6 thymi and co-cultured with apoptotic GFP^+ TA3 cells at a 1:1 ratio for 6 hours with either CD36 blocking antibody or vehicle. $CD11c^+$ I-Ab^+ $CD24^+$ DCs were analyzed for Eα presentation (Y-Ae^+ cells) acquired from TA3 cells via FACS. Shown are representative FACS plots and summary graph of three independent experiments. ***$p < .001$.

(D) Shown is experimental schematic and representative FACS plots. Thymi from congenic $Ly5.1^+$ B6 (C57BL/6) and Balb/c mice were harvested, split in half, and either digested by itself or with an allogeneic thymus. Thymus preps were stained for DC markers, Y-Ae, and I-A^d, and analyzed by flow cytometry. FACS plots are representative of two independent experiments with two replicates per condition. DC subsets were identified as per Methods.

(E) Representative FACS plots and summary graph of Eα presentation in $CD8\alpha^+$ DCs from C57BL/6→Balb/c BM chimeras treated with the pan-caspase inhibitor z-VAD-FMK for three days prior to harvest to inhibit apoptosis. Data are presented as mean + SD from two independent experiments with 1-2 replicates per condition. ***$p < .001$

(F) Representative FACS plots and summary graph of Eα presentation in $CD8\alpha^+$ DCs from C57BL/6→Balb/c BM chimeras treated with the purinergic receptor inhibitor Suramin for three days prior to harvest. Data are presented as mean + SD from two independent experiments with 1-2 replicates per condition. ***$p < .001$

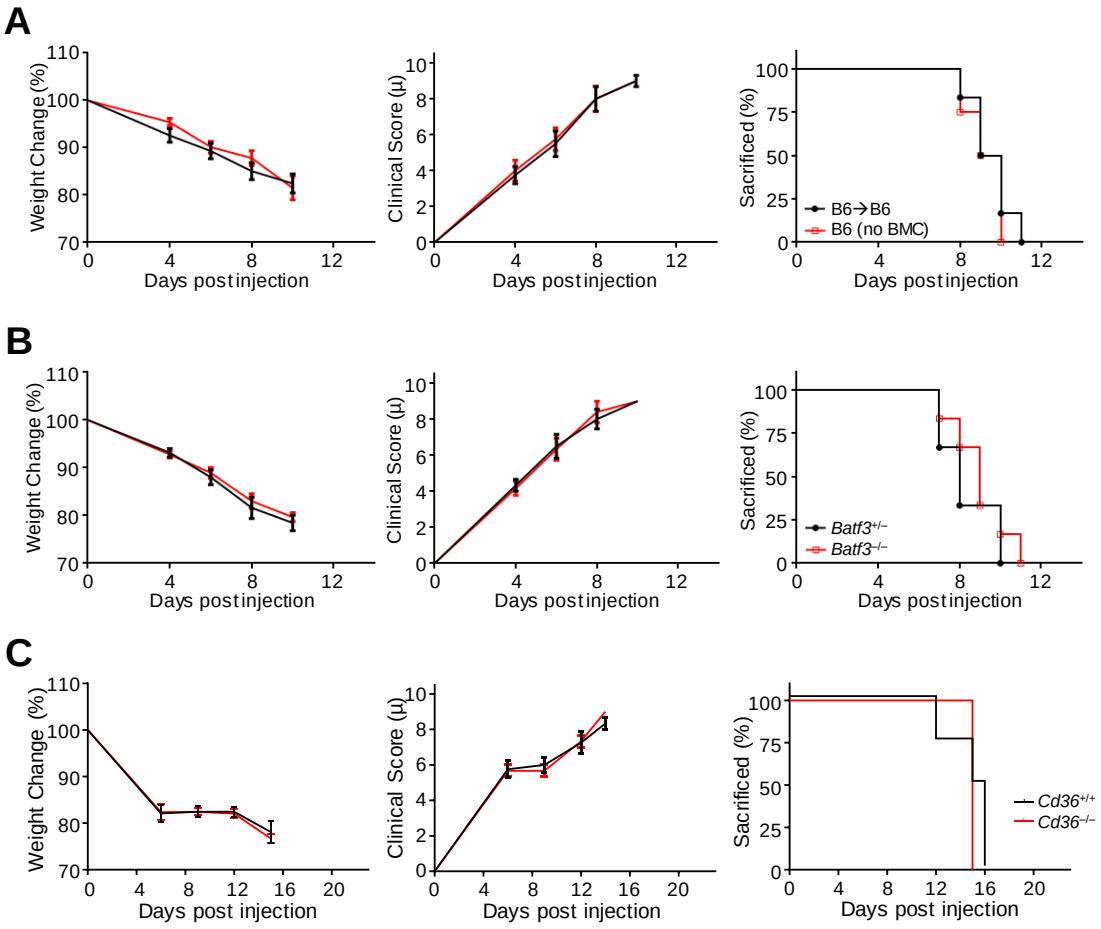

Figure S6. Related to Figure 6. BATF3 and CD36 are required for allo-tolerance development.

(A) Thymic CD4$^+$ Tconv cells were sorted directly from B6 mice versus syngeneic B6 → B6 BM chimeras to induce acute GVHD as per Figure 6A.

(B) Thymic CD4$^+$ Tconv cells from *Batf3*$^{+/–}$ and *Batf3*$^{–/–}$ mice were sorted used to induce acute GVHD as per Figure 6A.

(C) Thymic CD4+ Tconv cells from mixed BM chimera consisting of congenically labeled CD36 sufficient and deficient BM were sorted and used to induce acute GHVD as per Figure. 6A. Course of acute GVHD was determined by weight change, clinical score, and percent sacrificed. Summary plots are of one to three independent experiments with two to four mice per condition. Data are summarized as mean ± SEM.

A

ID	Sex	BMT Indication	Donor Type	HLA match grade	GVHD Symptoms	GVHD onset (days)	Last Follow-up (days)	Age at Collection (years)
R001	M	ALL	haplo-mother	5/10	Skin	267	739	21
R002	M	AML	haplo-sibling	4/6	GI	24	125	70
R003	F	AML	haplo-sibling	3/6	Lung	413	1989	32
R004	M	AML	haplo-sister	5/10	GI	68	210	38
R005	F	MDS	haplo-daughter	5/10	GI	34	64	67
R006	M	AML	haplo-father	5/10	Skin	154	1363	24
R007	M	AML	haplo-daughter	5/10	Skin	83	398	53
R008	M	AML	haplo-bother	2/4	Skin, Fever	27	130	68
R009	M	AML	haplo-unrelated	5/10	Skin, Liver, GI	32	501	36
R011	F	ALL	haplo-brother	2/4	no	N/A	361	27
R012	M	NHL	allo-sibling	4/6	no	N/A	1225	45
R013	F	AML	haplo-brother	4/6	no	N/A	402	32
R014	M	AML	haplo-sister	5/10	no	N/A	691	57
R015	M	AML	haplo-mother	5/10	no	N/A	550	42
R016	M	AML	haplo-unrelated	5/10	no	N/A	74	64
R017	M	AML	haplo-sister	5/10	no	N/A	207	25
R018	M	AML	haplo-son	5/10	no	N/A	361	65
R019	M	AML	haplo-son	5/10	no	N/A	67	67
R020	M	ALL	haplo-father	3/6	no	N/A	243	20

B

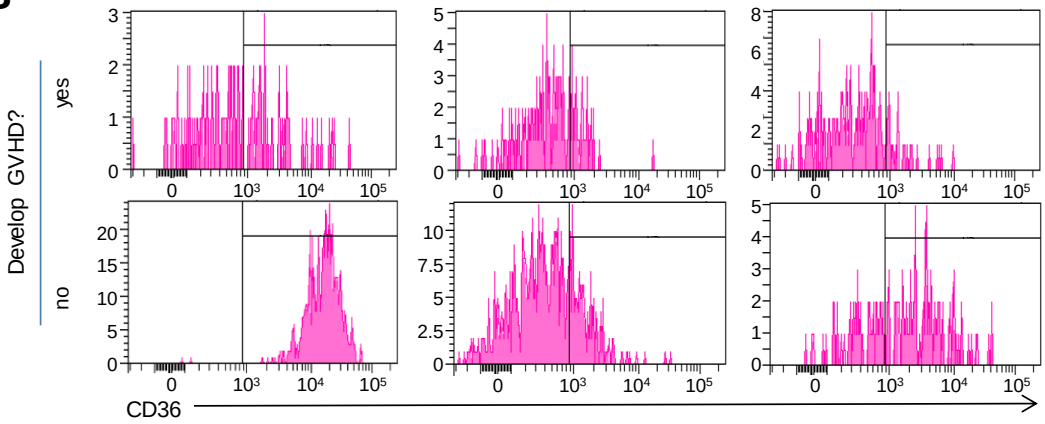

C

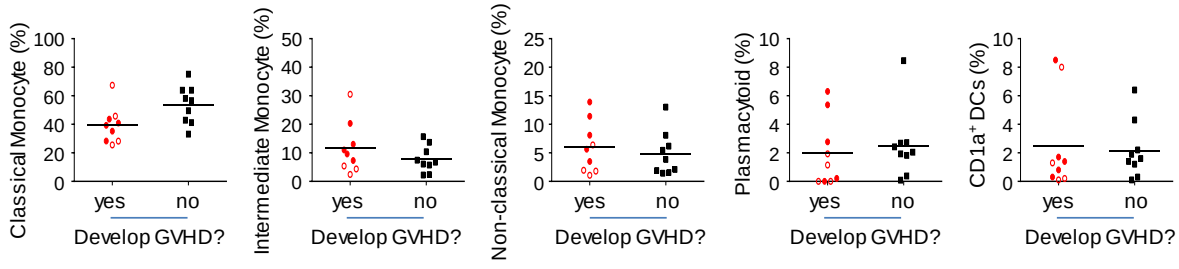

Figure S7. Related to Figure 7. Analysis of human peripheral blood mononuclear cell subsets in bone marrow transplantation patients.

(A) Demographic and clinical information of patients undergoing bone marrow transplantation relevant to Figure 7A. Blood was collected 30 days after bone marrow transplantation and PBMCs harvested via protocol described in Method. HLA match grade was determined by HLA typing of HLA-A, B, and DR from both alleles for sibling donors and of HLA-A, B, C, DR, and DQ from both alleles for non-sibling donors. GVHD onset represents the first self-reported symptom used in the diagnosis. Red values indicate dates greater than 30 days after the peripheral blood draw used for this analysis. Abbreviations used in table: ALL: Acute Lymphoblastic Leukemia, AML: Acute Myeloid Leukemia, MDS: Myelodysplastic Syndrome. NHL: Non-Hodgkin Lymphoma. GI: Gastrointestinal.

(B) CD36 expression on $CD141^{+}$ DCs. CD36 expression was gated based on isotype control. Three representative patients of each cGHVD status are shown.

(C) Characterization of PBMC subsets as in Figure 7A. Each dot represents an individual patient sample. Samples were pre-gated as $CD45^{+}$ $CD3^{-}$ $CD19^{-}$ $CD56^{-}$. These cells were then gated as $CD14^{++}$ $CD16^{-}$ (classical monocytes), $CD14^{++}$ $CD16^{+}$ (intermediate monocyte), and $CD14^{-}$ $CD16^{+}$ (non-classical monocyte). $CD14^{-}$ $CD16^{-}$ cells were then gated as HLA-DR^{+} $CD303^{+}$ (plasmacytoid DC), HLA-DR^{+} $CD1a^{+}$ ($CD1a^{+}$ DC) or HLA-DR^{+} $CD141^{+}$ ($CD141^{+}$ DC). Red dots indicate patients who self-reported cGVHD symptoms over 30 days after this peripheral blood draw.